Advances in Materials Research, *Vol. 6 No. 3 (2017) 279-301*
DOI: https://doi.org/10.12989/amr.2017.6.3.279

Thermo-mechanical vibration analysis of functionally graded micro/nanoscale beams with porosities based on modified couple stress theory

Farzad Ebrahimi *, Fateme Mahmoodi and Mohammad Reza Barati

Department of Mechanical Engineering, Faculty of Engineering,
Imam Khomeini International University, Qazvin, Iran

(*Received September 18, 2016, Revised September 6, 2017, Accepted December 3, 2017*)

Abstract. Thermo-mechanical vibration characteristics of in homogeneousporous functionally graded (FG) micro/nanobeam subjected to various types of thermal loadings are investigated in the present paper based on modified couple stress theory with consideration of the exact position of neutral axis. The FG micro/nanobeam is modeled via a refined hyperbolic beam theory in which shear deformation effect is verified needless of shear correction factor. A modified power-law distribution which contains porosity volume fraction is used to describe the graded material properties of FG micro/nanobeam. Temperature field has uniform, linear and nonlinear distributions across the thickness. The governing equations and the related boundary conditions are derived by Extended Hamilton's principle and they are solved applying an analytical solution which satisfies various boundary conditions. A comparison study is performed to verify the present formulation with the known data in the literature and a good agreement is observed. The parametric study covered in this paper includes several parameters such as thermal loadings, porosity volume fraction, power-law exponents, slenderness ratio, scale parameter and various boundary conditions on natural frequencies of porous FG micro/nanobeams in detail.

Keywords: free vibration; thermal effect; porosity; FG microbeam; modified couple stress theory

1. Introduction

Functionally graded materials (FGMs) are known as the great materials in mechanical properties, thermal and corrosive resistance. Due to the advances in manufacturing technology and extended behavior of FGM, researchers eager to study different behaviors of this material. For the first time, a group of Japanese scientists in the mid-1980s, introduced FGMs as a novel generation of heterogeneous composites and as thermal barrier materials in severe temperature environments. FGMs were recovered by controlling the volume fractions, microstructure, porosity, etc. of the material constituents during manufacturing, resulting in spatial gradient of macroscopic material properties (Ebrahimi and Rastgoo 2008).

Therefore, FGMs with a mixture of the ceramic and metal are applied to the thermal barrier structures for the space shuttle, combustion chamber and nuclear planets etc. (Ebrahimi *et al*. 2009,

*Corresponding author, Professor, E-mail: febrahimy@eng.ikiu.ac.ir

http://www.techno-press.org/?journal=amr&subpage=5 ISSN: 2234-0912 (Print), 2234-179X (Online)

Ebrahimi and Rastgoo 2009, 2011, Aghelinejad *et al*. 2011). In view of these advantages, a number of investigations, dealing with static, buckling, dynamic characteristics of functionally graded (FG) structures, had been published in the scientific literature. (Ebrahimi and Barati 2016a-e, Ebrahimi *et al*. 2016a, Ebrahimi and Dabbagh 2016, Ebrahimi and Hosseini 2016a, b). In the last decade, the trend of using beams and plates made of FGMs for engineering structures has significantly increased (Şimşek and Kocatürk (2009) – Thai and Vo (2012)). Therefore, understanding the behavior of structures made of porous FGMs subjected to a variety of mechanical and thermal loadings is very important for their accurate design.

Due to creation of micro voids or porosities inside FGMs during fabrication, the mechanical behavior of structural components made of such materials is influenced by the value of porosity volume fraction. The porous materials are composed of two elements, one of which is solid and the other is either liquid or gas and can be found in nature, such as wood and stone. Following this, for analysis of porous FG structures, a vibration analysis of layered functionally graded beams is conducted by Wattanasakulpong *et al*. (2012). They validated the obtained results with experimental results and reported that discrepancies between theoretical and experimental results could arise from porosities due to imperfect infiltration and from approximation in material profile in calculation. Also, Wattanasakulpong and Ungbhakorn (2014) studied vibration behavior of porous FGM beams with elastically restrained ends. They used a modified form of rule of mixture to illustrate the material properties of FG beam with porosities. Ebrahimi and Mokhtari presented the transverse vibration analysis of rotating porous FGM beams by using differential transform method (DTM) (Ebrahimi and Mokhtari 2015). Ebrahimi and Zia (2015) utilized the Galerkin and multiple scale methods to solve the motion equations of porous FG beams for the large amplitude nonlinear vibration analysis. Ebrahimi *et al*. (2016b) examined thermal effects on vibrational behavior of temperature-dependent FG Euler-Bernoulli beams with porosities employing differential transform method. In another study, Ebrahimi and Jafari (2016) investigated thermo-mechanical vibration characteristics of porous FG beams subjected to uniform, linear and nonlinear thermal loadings. They indicated that type of thermal loading as well as porosity volume fractions have a significant influence on vibration frequencies of porous FG beams.

With the quick expansion of technology, it is now substandard to use FG beams and plates in micro/nano electromechanical systems (MEMS/NEMS), electrically actuated MEMS devices and atomic force microscopes (AFMs) (Lü *et al*. (2009) - Hasanyan *et al*. (2008) - Ebrahimi *et al*. (2016a)-(2017)). It is obvious that classical continuum mechanics does not account for such size effects in micro, nanoscale structures. To eliminate this problem, the modified couple stress and the strain gradient elasticity theories have been widely handled to analysis the static and dynamic behavior of Microscale structures. Due to the experimentally determining of micro-structural material length scale parameters is difficult, Yang *et al*. (2002) have suggested the modified couple stress theory (MCST) in which the strain energy has been demonstrated to be a quadratic function of the strain tensor and the symmetric part of curvature tensor, and a length scale parameter is included (Yang *et al*. 2002). In this field, Asghari *et al*. (2010) investigated the size-dependent static and vibrational behavior of FG microbeams based on modified couple stress theory (Asghari *et al*. 2011). Nonlinear vibration of FG microbeams according to modified couple stress theory and von- Kármán geometric nonlinearity is studied by Ke *et al*. (2012). Şimşek *et al*. (2013) explored the static behavior FG microbeams based on Timoshenko beam model. Akgöz and Civalek (2013) researched vibration behavior of axially FG tapered microbeams based on the modified couple stress theory. Şimşek and Reddy (2013) proposed a higher order beam model for bending and vibration of FG microbeams using the modified couple stress theory. Also, Akgöz and Civalek

(2014) explored thermal buckling of FG microbeams embedded in elastic foundation. Al-Basyouni *et al*. (2015) presented a refined beam model for size-dependent bending and vibration analysis of FG microbeams based on neutral surface position. They stated that contrary to the other high order beam theories, their proposed transverse displacement is assumes both of bending and shear components and there is no need for any shear correction factor. So, the sinusoidal beam theory (SBT) together with the classical beam theory (CBT) can be easily created. They compared the results of classical, first order and sinusoidal beam theories in their work. Ghadiri and Shafiei (2016) conducted vibration analysis of rotating FG microbeams under different temperature distributions. Dehrouyeh-Semnani *et al*. (2016) examined free flexural vibration of geometrically imperfect functionally graded microbeams using a weighted-residual method. Ansari *et al*. (2016) investigated nonlinear mechanical behavior of third-order FG microbeams using the variational differential quadrature method. In the above mentioned papers concerning with analysis of FG microbeams, porosity effect was not considered. However, to the authors' best knowledge, no research dealing with influence of porosity distribution on the thermal vibration analysis of FGM microbeams with different boundary conditions. Actually, by exerting a high temperature environment to the FGM based structures, the material properties vary significantly. For instance, Young's modulus usually reduces due to temperature rise. For more precise prediction of FGMs response exposed to extreme temperatures, material properties should be dependent on temperature. Hence, it is crucial to investigate free vibration behavior of porous FG microbeam with temperature-dependent material properties subjected to different temperature fields.

In this paper, thermo-mechanical vibration behavior of FG microbeams with porosities is examined based on modified couple stress theory in conjunction with a higher-order refined theory. The model contains a hyperbolic shear strain function to capture the shear deformation effects. Also, the exact position of neutral axis is considered in this study to provide more accurate results. Three type of thermal loading called uniform, linear and nonlinear temperature rises are considered. The material properties of FG microbeam are estimated to vary in the thickness direction according to a modified power-law function. The governing differential equations of motion are derived by using Extended Hamilton's principle and an analytical solution is employed to solve the equations for various boundary conditions. The results of present study are compared with those of porous FG macro beams and also size-dependent FG microbeams without porosity effect. The influences of the various thermal loadings, porosity volume fraction, gradient index, slenderness ratio, scale parameter and different boundary conditions on natural frequencies of porous FG microbeam are investigated. The advantage of the present article is that the effects of various factors on vibration characteristics of FG micro/nanoscale beams with porosities are investigated in detail.

2. Theoretical formulation

2.1 Power-law functionally graded beams with porosities

In this paper a porous FG micro-scale beam with length of L and thickness h is supposed. Due to the reason that the material properties of FG beam are not symmetric with respect to the middle axis, the stretching and bending equations are coupled. Two different axis are considered for the measurement of z, namely z_{ms} and z_{ns} measured from the central axis and the neutral axis, respectively to determine the exact position of neutral axis of FG microbeam, as shown in Fig. 1. Based on the rule of mixture, the effective material properties, P_f, can be expressed by

$$P_f = P_c V_c + P_m V_m \tag{1}$$

Where P_c, P_m, V_c and V_m are the material properties and the volume-fraction of the metal and ceramic phases, respectively which are related by

$$V_c + V_m = 1 \tag{2}$$

And the volume-fraction of ceramic phase V_c is expressed as

$$V_c = \left(\frac{z_{ms}}{h} + \frac{1}{2}\right)^p = \left(\frac{z_{ns} + C}{h} + \frac{1}{2}\right)^p \tag{3}$$

Where the physical neutral axis of FG beams can be defined as a function of Láme's constants (λ and μ) as (Al-Basyouni 2015)

$$C = \frac{\int_{-\frac{h}{2}}^{\frac{h}{2}} [\lambda(z_{ms}) + 2\mu(z_{ms})] z_{ms}\, dz_{ms}}{\int_{-\frac{h}{2}}^{\frac{h}{2}} [\lambda(z_{ms}) + 2\mu(z_{ms})]\, dz_{ms}} \tag{4}$$

It is clear that distance (C) becomes zero for homogeneous microbeams. It is assumed in this paper that the FG microbeam has porosities spreading within the cross-section due to defect during production. Finally, the effective material properties such as Young's modulus (E), Poisson's ratio (ν), mass density (ρ), thermal conductivity (K), and thermal expansion coefficient (γ) can be expressed based on the modified power-law model as follows (Ebrahimi and Jafari 2016)

$$E(z_{ns}) = (E_c - E_m)\left(\frac{z_{ns} + C}{h} + \frac{1}{2}\right)^p + E_m + (E_c - E_m)\frac{\alpha}{2} \tag{5}$$

$$\rho(z_{ns}) = (\rho_c - \rho_m)\left(\frac{z_{ns} + C}{h} + \frac{1}{2}\right)^p + \rho_m + (\rho_c - \rho_m)\frac{\alpha}{2} \tag{6}$$

$$\nu(z_{ns}) = (\nu_c - \nu_m)\left(\frac{z_{ns} + C}{h} + \frac{1}{2}\right)^p + \nu_m + (\nu_c - \nu_m)\frac{\alpha}{2} \tag{7}$$

$$\gamma(z_{ns}) = (\gamma_c - \gamma_m)\left(\frac{z_{ns} + C}{h} + \frac{1}{2}\right)^p + \gamma_m + (\gamma_c - \gamma_m)\frac{\alpha}{2} \tag{8}$$

$$k(z_{ns}) = (k_c - k_m)\left(\frac{z_{ns} + C}{h} + \frac{1}{2}\right)^p + k_m + (k_c - k_m)\frac{\alpha}{2} \tag{9}$$

Where the subscripts of m, c denote the metal and ceramic constituents and α is the volume fraction of porosity. Also, the temperature-dependency of material properties can be defined using the following expression

$$P = P_0(P_{-1}T^{-1} + 1 + P_1 T + P_2 T^2 + P_3 T^3) \tag{10}$$

Where P_0 , P_1, P_2 and P_3 are material coefficients which can be seen in the Table 1 for SUS304 and Al_2O_3. The bottom surface of FGM beam is pure metal (SUS304), whereas the top surface is pure ceramic (Si_3N_4).

2.2 The modified couple stress theory

According to the modified couple stress model, the strain energy, U of an elastic material occupying region $\Omega$is related to the strain and curvature tensors as

$$U = \frac{1}{2}\int_{\Omega} (\sigma_{ij}\,\varepsilon_{ij} + m_{ij}\,\chi_{ij})dV \qquad (i.j = 1.2.3) \tag{11}$$

Where σ, ε, m and χ are Cauchy stress tensor, classical strain tensor, deviatoric part of the couple stress tensor and symmetric curvature tensor, respectively.

The strain and curvature tensors can be defined by

$$\varepsilon_{ij} = \frac{1}{2}(u_{i.j} + u_{j.i}) \tag{12}$$

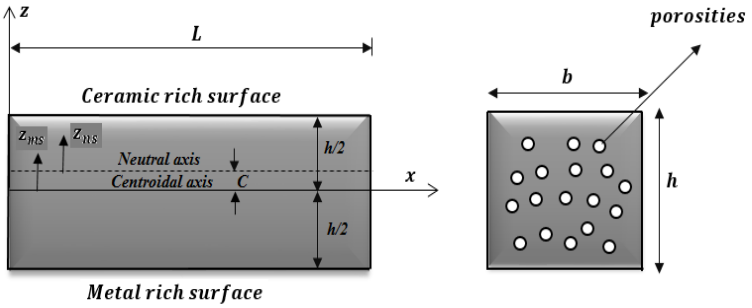

Fig. 1 The geometry and position of neutral axis for a FG microbeam with porosity

Table 1 Temperature-dependent coefficients for Si_3N_4 and SUS304 (Lee and Kim 2013)

Material	Properties	P_0	P_{-1}	P_1	P_2	P_3
Si_3N_4	E (Pa)	348.43e+9	0	-3.070e-4	2.160e-7	-8.946e-11
	γ (K^{-1})	5.8723e-6	0	9.095e-4	0	0
	ρ (Kg/m^3)	2370	0	0	0	0
	κ (W/mK)	13.723	0	-1.032e-3	5.466e-7	-7.876e-11
	ν	0.24	0	0	0	0
SUS304	E (Pa)	201.04e+9	0	3.079e-4	-6.534e-7	0
	γ (K^{-1})	12.330e-6	0	8.086e-4	0	0
	ρ (Kg/m^3)	8166	0	0	0	0
	κ (W/mK)	15.379	0	-1.264e-3	2.092e-6	-7.223e-10
	ν	0.3262	0	-2.002e-4	3.797e-7	0

$$\chi_{ij} = \frac{1}{2}(\theta_{i.j} + \theta_{j.i}) \tag{13}$$

Where u and θ are the components of the displacement and rotation vectors written by

$$\theta_i = \frac{1}{2} e_{ijk}\, u_{k.j} \tag{14}$$

In which e_{ijk} is the permutation symbol. The constitutive relations can be expressed as

$$\sigma_{ij} = \lambda(z_{ns})\epsilon_{kk}\,\delta_{ij} + 2\mu(z_{ns})\epsilon_{ij} \tag{15}$$

$$m_{ij} = 2\mu(z_{ns})[l(z_{ns})]^2 X_{ij} \tag{16}$$

Where δ_{ij} is the Kroenke delta, $l$is the material length scale parameter which reflects the effect of couple stress. Also, the Láme's constants can be defined by

$$\lambda(z_{ns}) = \frac{E(z_{ns})\nu(z_{ns})}{[1+\nu(z_{ns})][1-2\nu(z_{ns})]} \tag{17}$$

$$\mu(z_{ns}) = \frac{E(z_{ns})}{2[1+\nu(z_{ns})]} \tag{18}$$

2.3 The refined FGM microbeam model

The displacement field of FG microbeam according to the refined shear-deformable beam model can be expressed by (Al-Basyouni *et al*. 2015)

$$u_x(x, z_{ns}, t) = u_0(x,t) - z_{ns}\frac{\partial w_b}{\partial x} - f(z_{ns})\frac{\partial w_s}{\partial x} \tag{19}$$

$$u_y(x, z_{ns}, t) = 0 \tag{20}$$

$$u_z(x, z_{ns}, t) = w_b(x,t) + w_s(x,t) \tag{21}$$

In which u is displacement component of the mid-axis and w_b and w_s denote the bending and shear transverse displacement, respectively.

Also:

- For the classical beam theory (CBT)

$$w_s(x.t) = 0 \tag{22}$$

- For the first order beam theory (FBT)

$$f(z_{ns}) = 0 \tag{23}$$

- For the sinusoidal beam theory (SBT) (Al-Basyouni *et al*. 2015)

$$f(z_{ns}) = (z_{ns} + C) - \frac{h}{\pi}\sin\left(\frac{\pi(z_{ns} + C)}{h}\right) \tag{24}$$

- For the hyperbolic beam theory (HBT) (Şimşek *et al*. 2013)

$$f(z_{ns}) = \frac{\frac{h}{\pi}\sinh\left(\frac{\pi(z_{ns} + C)}{h}\right) - (z_{ns} + C)}{\cosh(\frac{\pi}{2}) - 1} \tag{25}$$

Finally, the non-zero strains of the present refined beam model are achieved as

$$\epsilon_x = \frac{\partial u_0}{\partial x} - z_{ns}\frac{\partial^2 w_b}{\partial x^2} - f(z_{ns})\frac{\partial^2 w_s}{\partial x^2} \tag{26}$$

$$\epsilon_y = \epsilon_z = \gamma_{xy} = \gamma_{yz} = 0 \tag{27}$$

$$\gamma_{xz} = 2\epsilon_{xz} = g(z_{ns})\frac{\partial w_s}{\partial x} \tag{28}$$

Where $g(z_{ns}) = 1 - f^{'}(z_{ns})$. In addition, Eqs. (12)-(13) and (14) give

$$\theta_y = -\frac{\partial w_b}{\partial x} - \frac{1}{2}\psi(z_{ns})\frac{\partial w_s}{\partial x}, \qquad \theta_x = \theta_z = 0 \tag{29}$$

With, $\psi(z_{ns}) = 1 + f^{'}(z_{ns})$

Substitution of Eq. (29) into (13) leads to the following expression for the non-zero components of the symmetric curvature tensor

$$X_{xy} = -\frac{1}{2}\frac{\partial^2 w_b}{\partial x^2} - \frac{1}{4}\psi(z_{ns})\frac{\partial^2 w_s}{\partial x^2}, \qquad X_{yz} = -\frac{1}{4}f^{''}(z_{ns})\frac{\partial w_s}{\partial x} \tag{30}$$

$$X_{xx} = X_{yy} = X_{zz} = X_{xz} = 0 \tag{31}$$

2.4 The governing equations

Governing equations of motions and boundary conditions for the free vibration of a FG micro-beam have been derived via Extended Hamilton's principle. The principle can be presented in analytical form as

$$\int_0^T \delta(U + V - K)dt = 0 \tag{32}$$

Here *U* is strain energy, *K* is kinetic energy and *V* is work done by external forces. δU is the virtual variation of the strain energy of the beam that can be stated as

$$\begin{aligned}\delta U &= \int_0^l \int_{-\frac{h}{2}-C}^{\frac{h}{2}-C} \left(\sigma_{ij}\,\delta\epsilon_{ij} + m_{ij}\,\delta X_{ij}\right) dz_{ns}\,dx \\ &= \int_0^l \int_{-\frac{h}{2}-C}^{\frac{h}{2}-C} \left(\sigma_x \delta\epsilon_x + \tau_{xz}\delta\gamma_{xz} + 2m\delta X_{xy} + 2m_{yz}\delta X_{yz}\right) dZ_{ns}\,dx \\ &= \int_0^l \left(N\frac{d\delta u_0}{dx} - (M_b + Y_1)\frac{d^2\delta w_b}{dx^2} - \left(M_s + \frac{1}{2}Y_1 + \frac{1}{2}Y_2\right)\frac{d^2\delta w_s}{dx^2} + \left(Q - \frac{1}{2}Y_3\right)\frac{d\delta w_s}{dx}\right) dx\end{aligned} \tag{33}$$

Where L is the length of the micro-scale beam, N is the axial force, M is the bending moment and Q is the shear force, the following stress resultants are presented as

$$(N.M_b.M_s) = \int_{-\frac{h}{2}-C}^{\frac{h}{2}-C} (1.z_{ns}.f)\sigma_x\,dz_{ns}, \qquad Q = \int_{-\frac{h}{2}-C}^{\frac{h}{2}-C} g\tau_{xz}\,dz_{ns} \tag{34}$$

$$(Y_1.Y_2) = \int_{-\frac{h}{2}-C}^{\frac{h}{2}-C} (1.f')m_{xy}\,dz_{ns}, \qquad Y_3 = \int_{-\frac{h}{2}-C}^{\frac{h}{2}-C} f''\,m_{yz}\,dz_{ns} \tag{35}$$

δV is the variation of work done by the external applied forces, that can be expressed as

$$\delta V = -\int_0^l N^T \frac{\partial(w_b + w_s)}{\partial x}\,\delta\left(\frac{\partial(w_b + w_s)}{\partial x}\right) dx \tag{36}$$

Where N^T is thermal resultant can be expressed as

$$N^T = \int_{-\frac{h}{2}-C}^{\frac{h}{2}-C} E(z_{ns}.T)\alpha(z_{ns}.T)\,(T - T_0)dz \tag{37}$$

The kinetic energy for present beam model can be expressed as

$$K = \frac{1}{2}\int_0^l \int_A \rho(z_{ns}.T)\left(\left(\frac{\partial u_x}{\partial t}\right)^2 + \left(\frac{\partial u_y}{\partial t}\right)^2 + \left(\frac{\partial u_z}{\partial t}\right)^2\right) dA dx \tag{38}$$

The variation of kinetic energy is written as

$$\delta K = \int_0^l \int_{-\frac{h}{2}-C}^{\frac{h}{2}-C} \rho(z_{ns}.T)[\dot{u}_x \delta\dot{u}_x + \dot{u}_z \delta\dot{u}_z]\, dz_{ns}\, dx$$
$$= \int_0^l \left\{ I_0[\dot{u}_0 \delta\dot{u}_0 + (\dot{w}_b + \dot{w}_s)(\delta\dot{w}_b + \delta\dot{w}_s)] - I_1\left(\dot{u}_0 \frac{d\delta\dot{w}_b}{dx} + \frac{d\dot{w}_b}{dx}\delta\dot{u}_0\right) + I_2\left(\frac{d\dot{w}_b}{dx}\frac{d\delta\dot{w}_b}{dx}\right) \right. \quad (39)$$
$$\left. - J_1\left(\dot{u}_0 \frac{d\delta\dot{w}_s}{dx} + \frac{d\dot{w}_s}{dx}\delta\dot{u}_0\right) + K_2\left(\frac{d\dot{w}_s}{dx}\frac{d\delta\dot{w}_s}{dx}\right) + J_2\left(\frac{d\dot{w}_b}{dx}\frac{d\delta\dot{w}_s}{dx} + \frac{d\dot{w}_s}{dx}\frac{d\delta\dot{w}_b}{dx}\right)\right\} dx$$

In which dot-superscript convention indicates the differentiation with respect to the time variable *t*; and ($I_0,\ I_1,\ J_1, I_2,\ J_2,\ K_2$) are the mass inertias determined as

$$(I_0.I_1.J_1.I_2.J_2.K_2) = \int_{-\frac{h}{2}-C}^{\frac{h}{2}-C} (1.z_{ns}.f.{z_{ns}}^2.z_{ns}f.f^2)\rho(z_{ns})dz_{ns} \quad (40)$$

Inserting the expressions for $\delta U,\ \delta V$ and δK from Eqs. (33), (36) and (39) into Eq. (32) andintegrating by parts versus both space and time variables, and collecting the coefficients of$\delta u_0, \delta w_b$ and w_s, the following equations of motion of the FG microbeam are obtained

$$\delta u_0 : \frac{dN}{dx} = I_0\ddot{u}_0 - I_1\frac{d\ddot{w}_b}{dx} - J_1\frac{d\ddot{w}_s}{dx} \quad (41)$$

$$\delta w_b : \frac{d^2M_b}{dx^2} + \frac{d^2Y_1}{dx^2} + q + N^T(\ddot{w}_b + \ddot{w}_s) = I_0(\ddot{w}_b + \ddot{w}_s) + I_1\frac{d\ddot{u}_0}{dx} - I_2\frac{d^2\ddot{w}_b}{dx^2} - J_2\frac{d^2\ddot{w}_s}{dx^2} \quad (42)$$

$$\delta w_s : \frac{d^2M_s}{dx^2} + \frac{1}{2}\frac{d^2Y_1}{dx^2} + \frac{1}{2}\frac{d^2Y_2}{dx^2} - \frac{1}{2}\frac{dY_3}{dx} + \frac{dQ}{dx} + q + N^T(\ddot{w}_b + \ddot{w}_s)$$
$$= I_0(\ddot{w}_b + \ddot{w}_s) + J_1\frac{d\ddot{u}_0}{dx} - J_2\frac{d^2\ddot{w}_b}{dx^2} - K_2\frac{d^2\ddot{w}_s}{dx^2} \quad (43)$$

And the following boundary conditions are obtained at *x* = 0 and *x* = *L*.

$$\text{Specify} \qquad u_o \ \text{ or } \ N \quad (44)$$

Specify

$$w_b \text{ or } V_b = \frac{dM_b}{dx} + \frac{dY_1}{dx} - I_1\ddot{u}_0 + I_2\frac{d\ddot{w}_b}{dx} + J_2\frac{d\ddot{w}_s}{dx} + N^T\frac{d(w_b + w_s)}{dx} - I_0\frac{d(w_b + w_s)}{dx} \quad (45)$$

Specify

$$w_s \text{ or } V_s = \frac{dM_s}{dx} + \frac{1}{2}\frac{dY_1}{dx} + \frac{1}{2}\frac{dY_2}{dx} - \frac{1}{2}Y_3 + Q - J\ddot{u}_0 + J_2\frac{d\ddot{w}_b}{dx} + K_2\frac{d\ddot{w}_s}{dx} + N^T\frac{d(w_b + w_s)}{dx} - I_0\frac{d(w_b + w_s)}{dx} \tag{46}$$

$$\text{Specify} \quad \frac{dw_b}{dx} \quad \text{or} \quad M_b + Y_1 + N^T - I_0 \tag{47}$$

$$\text{Specify} \quad \frac{dw_s}{dx} \quad \text{or} \quad M_s + \frac{1}{2}Y_1 + \frac{1}{2}Y_2 + N^T - I_0 \tag{48}$$

By employing Eqs. (34)-(35) and (41)- (42) and (43) the equations of motion of FG microbeam in terms of the displacements are calculated as

$$A_{11}\frac{d^2u_0}{dx^2} - B_{11}^s\frac{d^3w_s}{dx^3} = I_0\ddot{u}_0 - I_1\frac{d\ddot{w}_b}{dx} - J_1\frac{d\ddot{w}_s}{dx} - (D_{11} + A_{13})\frac{d^4w_b}{dx^4} \tag{49}$$

$$-\left(D_{11}^s + \frac{1}{2}(A_{13} + B_{13})\right)\frac{d^4w_s}{dx^4} + q + N^T(\ddot{w}_b + \ddot{w}_s) = I_0(\ddot{w}_b + \ddot{w}_s) + I_1\frac{d\ddot{u}_0}{dx} - I_2\frac{d^2\ddot{w}_b}{dx^2} - J_2\frac{d^2\ddot{w}_s}{dx^2} \tag{50}$$

$$B_{11}^s\frac{d^3u_0}{dx^3} - \left(D_{11}^s + \frac{1}{2}(A_{13} + B_{13})\right)\frac{d^4w_b}{dx^4} - \left(H_{11}^s + \frac{1}{4}(A_{13} + 2B_{13} + D_{13})\right)\frac{d^4w_s}{dx^4} + \left(A_{55}^s + \frac{1}{4}E_{13}\right)\frac{d^2w_s}{dx^2} + q + N^T(\ddot{w}_b + \ddot{w}_s) = I_0(\ddot{w}_b + \ddot{w}_s) + J_1\frac{d\ddot{u}_0}{dx} - J_2\frac{d^2\ddot{w}_b}{dx^2} - K_2\frac{d^2\ddot{w}_s}{dx^2} \tag{51}$$

Where A_{11}, B_{11}^s, etc., are the beam stiffness, defined by

$$(A_{11}.D_{11}.B_{11}^s.D_{11}^sH_{11}^s) = \int_{-\frac{h}{2}-C}^{\frac{h}{2}-C}\lambda(z_{ns})\frac{1-\nu(Z_{ns})}{\nu(Z_{ns})}(1.z_{ns}^2.f.z_{ns}f.f^2)dz_{ns} \tag{52}$$

$$(A_{13}.B_{13}.D_{13}.E_{13}) = \int_{-\frac{h}{2}-C}^{\frac{h}{2}-C}\mu(z_{ns})[l(z_{ns})]^2[1.f'.(f')^2.(f'')^2]dz_{ns} \tag{53}$$

$$A_{55}^{s} = \int_{-\frac{h}{2}-C}^{\frac{h}{2}-C} \mu(z_{ns}) g^2 dz_{ns} \tag{54}$$

3. Solution method

Here, an analytical solution of the governing equations is employed for free vibration porous FG microbeam under three types of boundary conditions (S-S, C-S and C-C).

- Simply-supported (S):

$w_b = w_s = M = 0 \quad \text{at} \quad x = 0\,, L$

- Clamped (C):

$u = w_b = w_s = 0 \quad \text{at} \quad x = 0\,, L$

Thus, the following expansions of displacements are supposed as

$$\begin{Bmatrix} u_0 \\ w_b \\ w_s \end{Bmatrix} = \sum_{n=1}^{\infty} \begin{Bmatrix} U_n \dfrac{\partial X_m(x)}{\partial x} e^{i\omega t} \\ W_{bn}\, X_m(x)\, e^{i\omega t} \\ W_{sn}\, X_m(x)\, e^{i\omega t} \end{Bmatrix} \tag{55}$$

Where, U_n, W_{bn} and W_{sn} are Fourier coefficients and ω is the eigenfrequency associated with *n*th eigen mode. Substituting Eq. (55) into Eq. (49)-(50) and (51) leads to

$$\left(\begin{bmatrix} S_{11} & 0 & S_{13} \\ 0 & S_{22} & S_{23} \\ S_{13} & S_{23} & S_{33} \end{bmatrix} - \omega^2 \begin{bmatrix} m_{11} & m_{12} & m_{13} \\ m_{12} & m_{22} & m_{23} \\ m_{13} & m_{23} & m_{33} \end{bmatrix} \right) \begin{Bmatrix} U_n \\ W_{bn} \\ W_{sn} \end{Bmatrix} = \{0\} \tag{56}$$

Where

$$\begin{gathered} S_{11} = A_{11}\beta_3, \quad S_{13} = -B_{11}^{s}\beta_9, \quad S_{22} = (D_{13} + A_{13})\beta_9 - N^T\beta_7 \\ S_{23} = \left(D_{11}^{s} + \frac{1}{2}(A_{13} + B_{13}) \right)\beta_9 + N^T\beta_7 \\ S_{33} = \left(H_{11}^{s} + \frac{1}{2}\left(B_{13} + \frac{1}{2}(D_{13} + A_{13}) \right) \right)\beta_9 + \left(A_{55}^{s} + \frac{1}{4}E_{13} + N^T \right)\beta_7 \end{gathered} \tag{57}$$

$$\begin{gathered} m_{11} = I_0\beta_1, \quad m_{12} = -I_1\beta_1, \quad m_{13} = -J_1\beta_7, \\ m_{22} = I_0\beta_5 + I_2\beta_7, \quad m_{23} = I_0\beta_5 + J_2\beta_7, \quad m_{32} = I_0\beta_5 + K_2\beta_7 \end{gathered} \tag{58}$$

In which

$$(\beta_1.\beta_3.\beta_5.\beta_7.\beta_9) = \int_0^L (X_m' X_m'.X_m X_m'''.X_m X_m.X_m'' X_m.X_m'''' X_m)\, dx \tag{59}$$

The function X_m for different boundary conditions is defined by

S-S:

$$X_m(x) = \sin(\lambda_n x)$$
$$\lambda_n = \frac{n\pi}{L} \tag{60}$$

C-C:

$$X_m(x) = \sin(\lambda_n x) - \sinh(\lambda_n x) - \xi_m(\cos(\lambda_n x) - \cosh(\lambda_n x))$$
$$\xi_m = \frac{\sin(\lambda_n x) - \sinh(\lambda_n x)}{\cos(\lambda_n x) - \cosh(\lambda_n x)} \tag{61}$$
$$\lambda_n = \frac{(n+0.5)n}{L}$$

C-S:

$$X_m(x) = \sin(\lambda_n x) - \sinh(\lambda_n x) - \xi_m(\cos(\lambda_n x) - \cosh(\lambda_n x))$$
$$\xi_m = \frac{\sin(\lambda_n x) + \sinh(\lambda_n x)}{\cos(\lambda_n x) + \cosh(\lambda_n x)} \tag{62}$$
$$\lambda_n = \frac{(n+0.25)n}{L}$$

4. Various types of thermal loading

4.1 Uniform temperature rise (*UTR*)

In this case, the FG microbeam initial temperature is assumed to be $T_0 = 300$ and uniformly changes to a final temperature of *T*. The temperature rise through the thickness direction is defined by

$$\Delta T = T - T_0 \tag{63}$$

4.2 Linear temperature rise (*LTR*)

In this case, the temperature of the top surface is T_c and it is considered to change linearly along the thickness to the bottom surface temperature, T_m. Hence, the temperature profile as a function of thickness is obtained as (Barati *et al*. (2016) - Kiani (Kiani and Eslami 2013))

$$T = T_m + \Delta T\left(\frac{1}{2} + \frac{z_{ns} + C}{h}\right) \tag{64}$$

4.3 Nonlinear temperature rise (*NLTR*)

The steady-state one dimensional heat conduction equation with the known temperature boundary conditions on bottom and top surfaces of the FG microbeam can be obtained by solving

the following equation (Ebrahimi and Jafari 2016)

$$-\frac{d}{dz}\left(k(z_{ns}.T)\frac{dT}{dz}\right)=0$$
$$T\left(\frac{h}{2}-C\right)=T_c \quad . \quad T\left(-\frac{h}{2}-C\right)=T_m \tag{65}$$

The solution of Eq. (55) subjected to the boundary conditions can be solved by the following equation

$$T=T_m+\Delta T\frac{\int_{-\frac{h}{2}-C}^{z_{ns}}\frac{1}{k(z_{ns}.T)}dz}{\int_{-\frac{h}{2}-C}^{\frac{h}{2}-C}\frac{1}{k(z_{ns}.T)}dz} \tag{66}$$

Where, $\Delta T=T_c-T_m$.

5. Numerical results and discussions

In this section, the effect of different temperature rises, porosity volume fraction, length scale parameter, slenderness ratio and boundary conditions on the natural frequencies of porous FG microbeam will be explored. It is assumed that the temperature increase in metal surface to reference temperature T_0 of the FGM microbeam is $T_m-T_0=5K$. The scale parameter in this study is taken as $l=15\,\mu m$. the following relation is accomplished in order to compute the non-dimensional natural frequencies

$$\bar{\omega}=\frac{\omega L^2}{h}\sqrt{\frac{\rho_c}{E_c}} \tag{67}$$

The validation study is carried out in two parts. First the results are validated with those of porous FG macro beams, and then they are validated with those of FG microbeams. Table 2

Table 2 Comparison of the non-dimensional natural frequency for porous FG beam under uniform temperature rise with various gradient indices (ΔT = 20)

B.C.		$p=0.1$		$p=0.2$		$p=0.5$	
		Ebrahimi *et al.* (2016b)	Present	Ebrahimi *et al.* (2016b)	Present	Ebrahimi *et al.* (2016b)	Present
S-S	$\alpha=0$	4.6536	4.61306	4.3867	4.35032	3.8974	3.8686
	$\alpha=0.1$	4.8339	4.79159	4.5215	4.48397	3.9598	3.92528
	$\alpha=0.2$	5.0693	5.02443	4.6925	4.65326	4.0328	4.00373
C-C	$\alpha=0$	10.8800	10.6858	10.2835	10.1045	9.1879	9.03596
	$\alpha=0.1$	11.2496	11.0504	10.5501	10.3685	9.2904	9.13965
	$\alpha=0.2$	11.7437	11.5371	10.8984	10.7126	9.417	9.26731

Table 3 Comparison of the non-dimensional natural frequency for a S–S FG micro-beam with various gradient indices ($h/l = 2$)

L/h	Beam theory	Gradient index			
		$p = 0.3$	$p = 1$	$p = 3$	$p = 10$
10	CBT (Al-Basyouni *et al*. 2015)	7.9307	6.6159	5.7362	5.1231
	FBT (Al-Basyouni *et al*. 2015)	7.8233	6.5211	5.6383	5.0237
	SBT (Al-Basyouni *et al*. 2015)	7.8722	6.5670	5.6876	5.0731
	Present	7.8720	6.5666	5.6876	5.0716
100	CBT (Al-Basyouni *et al*. 2015)	7.9651	6.6471	5.7633	5.1453
	FBT (Al-Basyouni *et al*. 2015)	7.9640	6.6461	5.7623	5.1442
	SBT (Al-Basyouni *et al*. 2015)	7.9645	6.6466	5.7628	5.1448
	Present	7.9641	6.6466	5.7628	5.1450

presented the comparison of the natural frequency of a porous FG beam under uniform temperature rise with those presented by Ebrahimi *et al*. (2016a) using differential transform method and Euler-Bernoulli beam model. Table 3 compares the results of the present study for S-S FG microbeams and the results presented by Al-Basyouni *et al*. (2015). In this case, the effects of temperature distributions and porosity volume fraction are omitted. According to this table, the results are presented for different power-law exponent, slenderness ratio and beam theories (CBT, FBT, SBT and HBT) and a good agreement is observed.

Table 4 presents the non-dimensional natural frequencies of porous FG microbeams subjected to uniform (UTR), linear (LTR) and nonlinear temperature rises (NLTR) under different boundary conditions (S-S, C-S and C-C) for various values of the volume fraction of porosity ($\alpha = 0, 0.1, 0.2$) and temperature changes ($\Delta T = 20/40/80$) at $L/h = 10$, $l/h = 2$ and $p = 1$. It is noticed that for all boundary conditions and thermal loadings, an increase in the temperature leads to smaller natural frequencies. It is evident that increasing the porosity parameter yields the growth in dimensionless frequencies for all types of thermal loading which highlights the

Table 4 Variation of the first non-dimensional frequency of S-S FG pouros microbeam for various porosity volume fraction, temperature, thermal loading, and boundary conditions ($p = 1, h/l = 2, L/h = 10$)

Boundary condition	Load Type	$\alpha = 0$			$\alpha = 0.1$			$\alpha = 0.2$		
		ΔT = 20	ΔT = 40	ΔT = 80	ΔT = 20	ΔT = 40	ΔT = 80	ΔT = 20	ΔT = 40	ΔT = 80
S-S	UTR	2.65833	2.64379	2.61235	2.76034	2.74561	2.71387	2.87074	2.85583	2.82378
	LTR	2.66282	2.65641	2.64215	2.76486	2.75837	2.74398	2.8753	2.86871	2.85421
	NLTR	2.66276	2.65635	2.64225	2.76481	2.75832	2.74411	2.87526	2.86868	2.85438
C-S	UTR	4.13143	4.11758	4.0872	4.2899	4.27581	4.24504	4.46138	4.44705	4.41589
	LTR	4.13611	4.13036	4.11697	4.2946	4.2887	4.27511	4.4661	4.46006	4.44628
	NLTR	4.13606	4.1303	4.11707	4.29455	4.28866	4.27525	4.46606	4.46003	4.44646
C-C	UTR	5.90382	5.89078	5.86149	6.13039	6.11704	6.08727	6.37555	6.36189	6.33165
	LTR	5.90874	5.90376	5.89136	6.13531	6.13012	6.11744	6.38048	6.37508	6.36212
	NLTR	5.90869	5.9037	5.89146	6.13526	6.13007	6.11758	6.38044	6.37505	6.36230

Table 5 Variation of the first non-dimensional frequency of S-S FG pouros microbeam for various scale parameter, temperature, thermal loading, and boundary conditions ($p = 1, \alpha = 0.2,\ L/h = 10$)

Boundary condition	Load Type	$\alpha = 0$			$\alpha = 0.1$			$\alpha = 0.2$		
		ΔT = 20	ΔT = 40	ΔT = 80	ΔT = 20	ΔT = 40	ΔT = 80	ΔT = 20	ΔT = 40	ΔT = 80
C-C	UTR	4.53254	4.52373	4.50396	2.87074	2.85583	2.82378	2.44148	2.42371	2.38572
	LTR	4.5356	4.53198	4.52306	2.87530	2.86871	2.85421	2.44677	2.43884	2.42167
	NLTR	4.53558	4.53196	4.52317	2.87526	2.86868	2.85438	2.44673	2.43881	2.42187
C-C	UTR	7.0483	7.04021	7.0212	4.46138	4.44705	4.41589	3.79242	3.77521	3.73823
	LTR	7.05157	7.04861	7.0403	4.4661	4.46006	4.44628	3.79788	3.79047	3.7741
	NLTR	7.05154	7.04859	7.04041	4.46606	4.46003	4.44646	3.79783	3.79043	3.7743
C-C	UTR	10.0869	10.0797	10.0616	6.37555	6.36189	6.33165	5.41396	5.39737	5.36135
	LTR	10.0904	10.0883	10.0807	6.38048	6.37508	6.36212	5.41962	5.41282	5.39733
	NLTR	10.0904	10.0883	10.0808	6.38044	6.37505	6.36230	5.41957	5.41278	5.39753

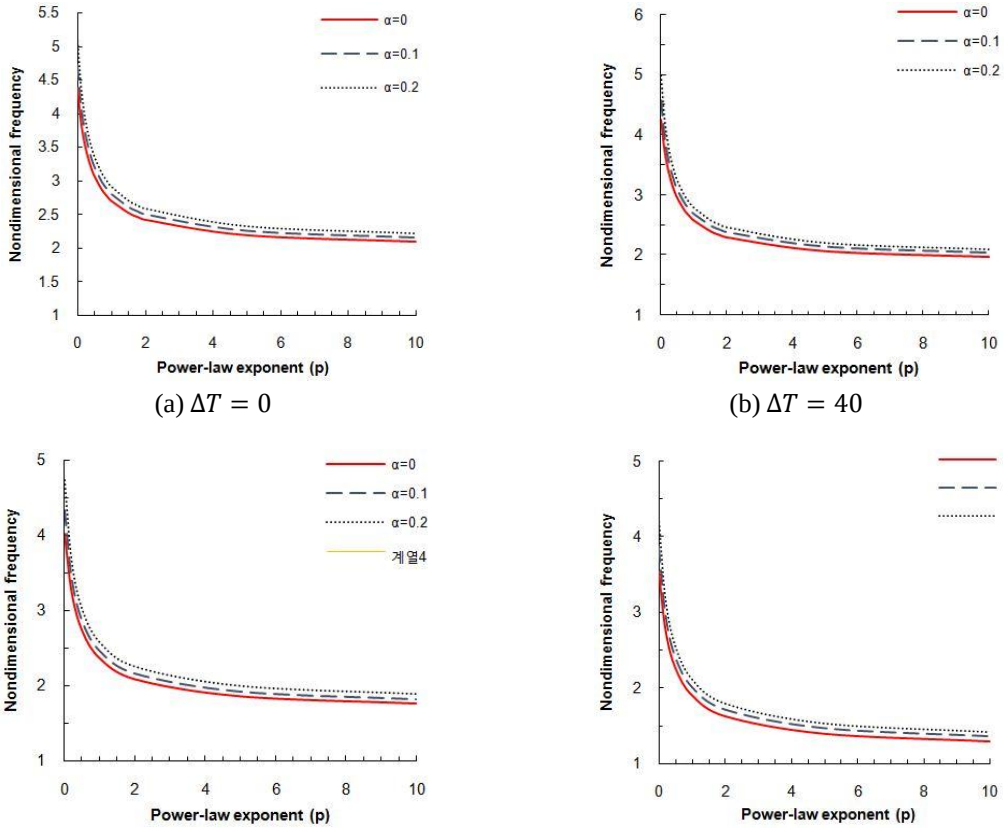

(a) $\Delta T = 0$ (b) $\Delta T = 40$

(c) $\Delta T = 100$ (d) $\Delta T = 200$

Fig. 2 Variation of the dimensionless frequency of S-S FG microbeam with material graduation and porosity for differentuniform temperature rises $(L/h = 20\ , h/l = 2)$

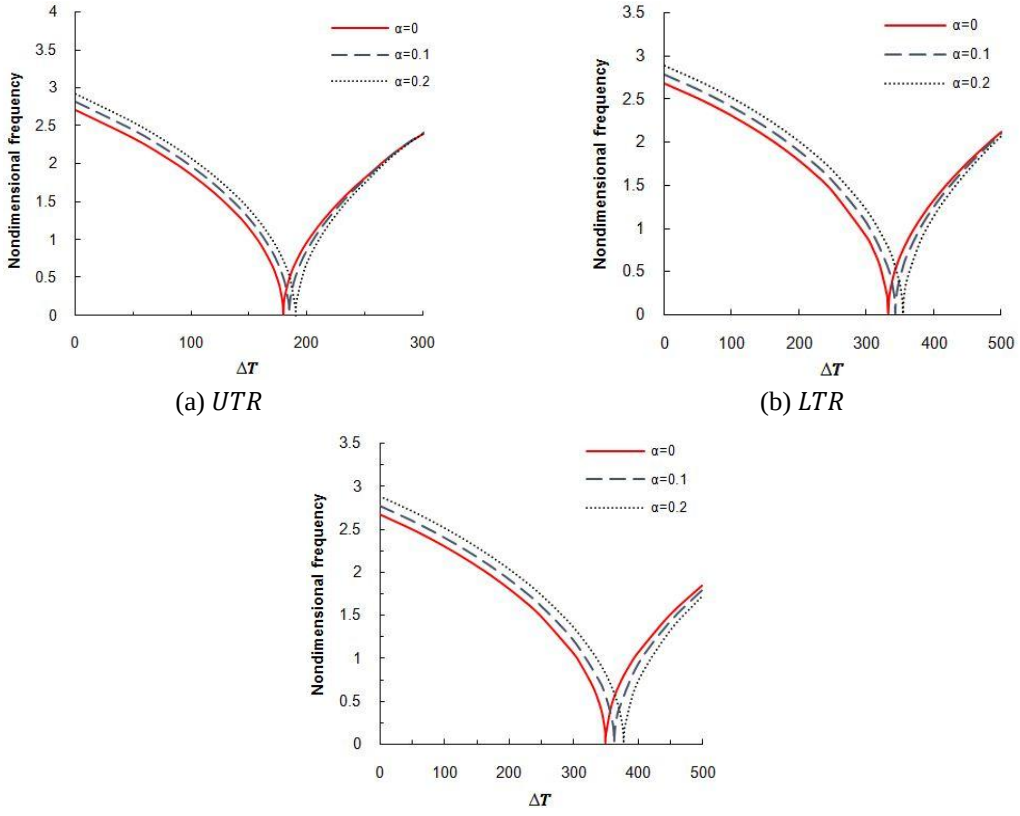

(a) UTR (b) LTR

(c) $NLTR$

Fig. 3 Variation of dimensionless frequency of S–S porous FG microbeam versus temperature changes for various values of porosity volume fraction ($L/h = 30,\ h/l = 2,\ p = 1$)

importance of the porosity effect on vibration behavior of FG microbeams. Also, it can be observed that the dimensionless natural frequencies according to UTR are minimum among all types of thermal loadings and the natural frequencies for LTR are maximum. So, vibration behavior of FG microbeams is significantly affected by the type of thermal loading, value of temperature change and also porosity distribution.

Table 5 presents the dimensionless frequency as a function of length scale parameter (h/l) and temperature change for different boundary conditions at $p = 1, \alpha = 0.2,\ L/h = 10$. It is revealed that at a constant porosity volume fraction (α), increasing length scale parameter leads to reduction in vibration frequencies of FG microbeams. Therefore, size effect plays a major role on vibration behavior of porous FG microbeams. Also, it is observable from this table that a porous FG microbeam with C-C boundary conditions possesses larger frequencies than C-S microbeams and the later has larger frequencies than those with S-S boundary conditions, regardless of thermal loading type. This is due to the fact that stronger supports at ends make the microbeam more rigid and vibration frequencies increases.

Fig. 2 shows the variation of the dimensionless frequency of simply-supported porous FG microbeam under uniform temperature rise with power-law exponent (p) for different porosity volume fractions at L/h = 20, h/l = 2. Various values of temperature change are considered in this

figure as ΔT = 0/40/100/200. It is observed that at a fixed porosity volume fraction, an increment in the power-law exponent leads to decreasing the dimensionless natural frequency. Such behavior is more announced at lower power-law exponents. This is due to the reason that by increasing the value of power-law exponent, the percentage of metal phase will rise, thus makes such FGM microbeams less rigid. Moreover, frequency decrement with respect to power-law exponent depends on the magnitude of porosity volume fraction. Growth of porosity volume fraction increases the natural frequencies for every value of power-law exponent and temperature change.

The variation of dimensionless natural frequencies of S–S and C-C FG microbeam subjected to three cases of thermal loadings (UTR, LTR and NLTR) for different porosity volume fraction and temperature changes at constant slenderness ratio L/h = 30, scale parameter h/l = 2 and power-law exponent p = 1 is depicted in Figs. 3 and 4. It is observed from the results of these figures that the dimensionless frequencies of porous FG microbeam decrease with the increment of temperature until it reaches to zero at the critical temperature point. This is due to stiffness reduction of microbeam with the rise of temperature. After the critical point, temperature increment gives larger frequencies at a constant porosity volume fraction. One significant observation within the range of temperature before the critical temperature is that the FG microbeams with larger values of porosity parameter possess higher frequency results. But, this trend is opposite in the range of

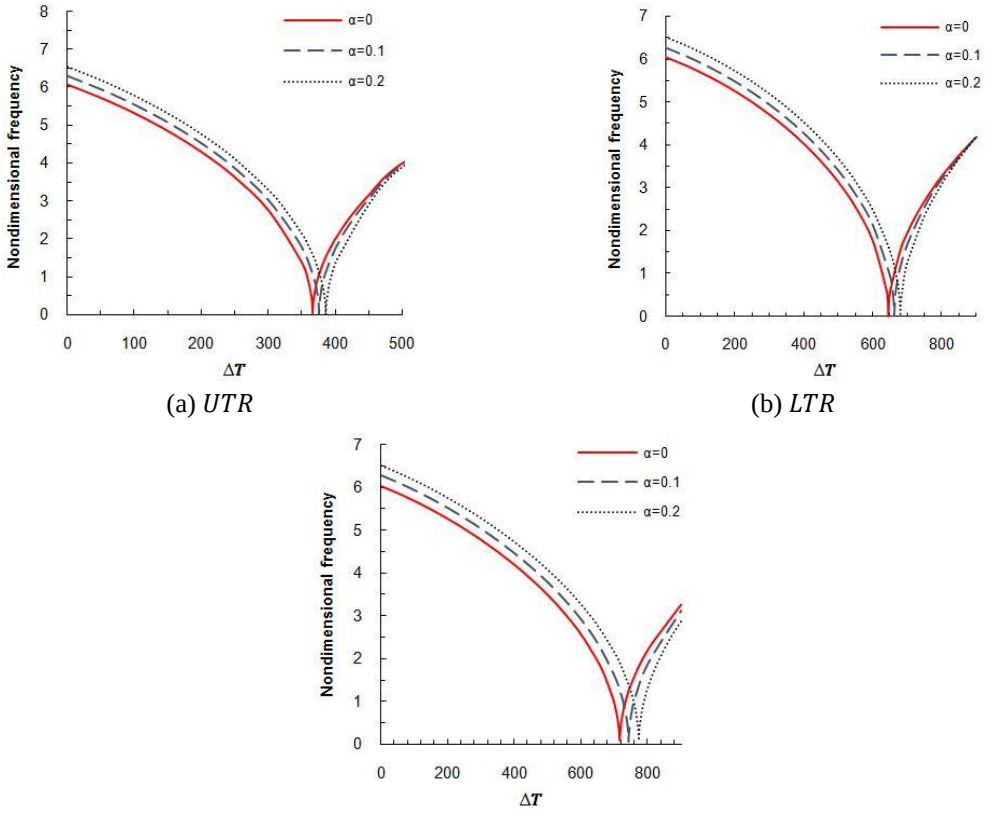

(a) UTR (b) LTR

(c) $NLTR$

Fig. 4 Variation of the dimensionless frequency of C–C FG porous microbeam with respect to various temperature rises for different values of porosity volume fraction ($L/h = 30,\ h/l = 2,\ p = 1$)

temperature further the critical point. So, larger values of porosity volume fraction provide larger critical temperatures for every kind of thermal loading. Also, it can be concluded that the critical temperature according to nonlinear temperature rise (NLTR) is larger than that of UTR and LTR for every value of porosity volume fraction. In addition, for every kind of thermal loading the critical temperatures of C-C porous FG microbeam is higher than those of S-S FG microbeams.

In Fig. 5, variation of the dimensionless frequency of S-S FG porous microbeam versus porosity volume fraction for various length scale parameters and temperature rises is illustrated at ΔT = 100, L/h = 10, $p = 1$. It is visible from this figure that the magnitudes of natural frequencies become smaller as the length scale parameter increases. This indicates that generally, natural frequencies increase with increasing in the porosity coefficient due to enhancement of FG microbeam structure.

The influence of porosity volume fraction and boundary condition on non-dimensional frequency of a FG microbeam subjected to three cases of temperature rise at ΔT = 100, L/h = 10, $h/l = 2$, $p = 1$ is demonstrated in Fig. 6. As expected, increasing the number of constraints at edges makes the microbeam stiffer and vibration frequencies increase. So, at a fixed temperature change and porosity volume fraction, the results of porous FG microbeam obey the following relation: C-C > C-S > S-S. Also, it is found that effect of porosity volume fraction on vibration

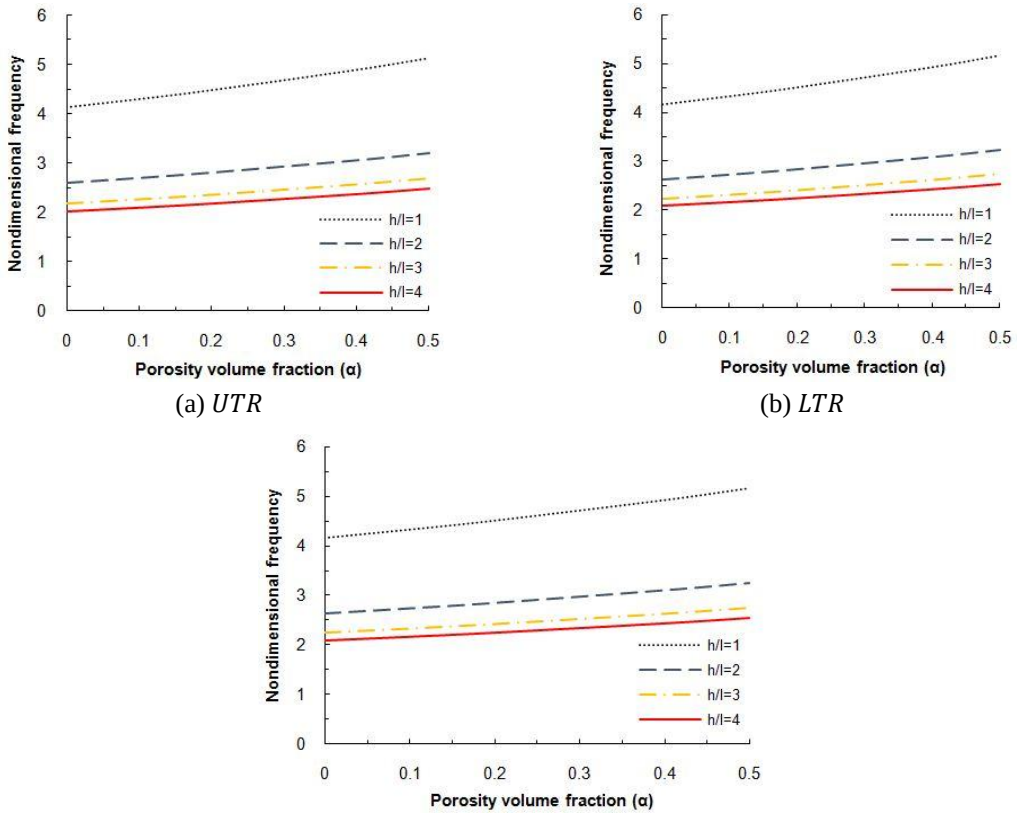

(a) UTR (b) LTR

(c) $NLTR$

Fig. 5 Variation of the dimensionless frequency of S-S FG porous microbeam versus porosity volume fraction for various scale parameters and temperature rises (ΔT = 100, L/h = 10, $p = 1$)

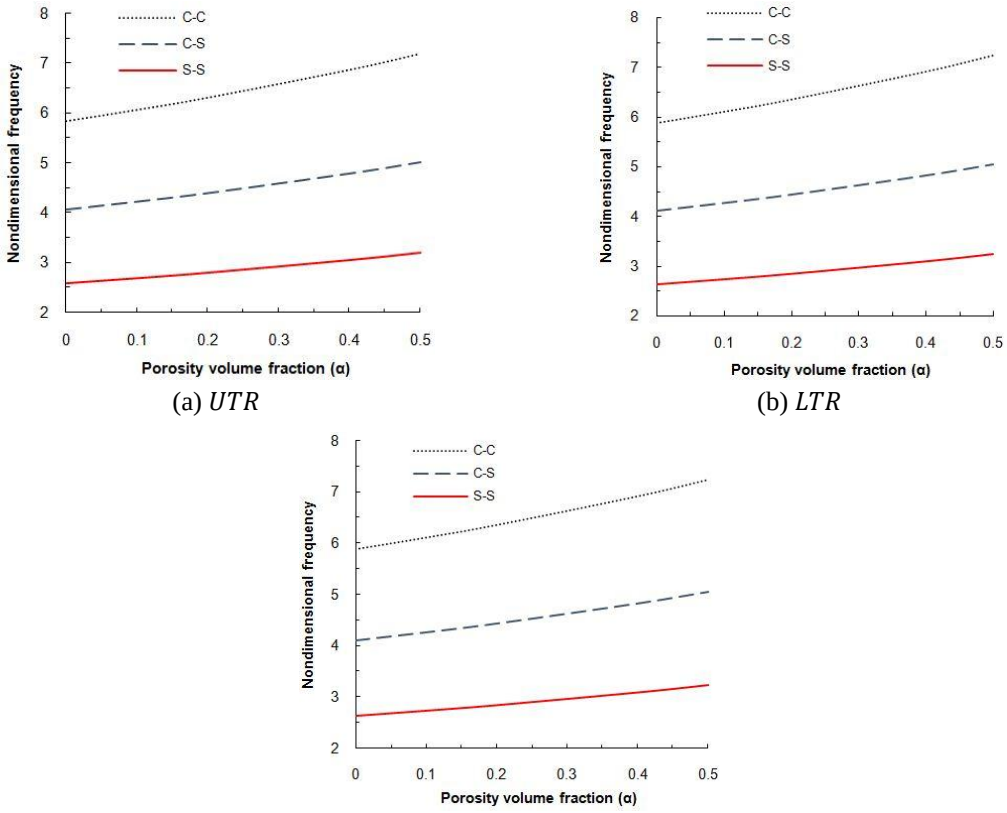

(a) UTR (b) LTR

(c) $NLTR$

Fig. 6 The variation of the dimensionless frequency of FG porous microbeam versus porosity volume fraction for different temperature rises and boundary conditions (ΔT = 100, L/h = 10, $h/l = 2,\ p = 1$)

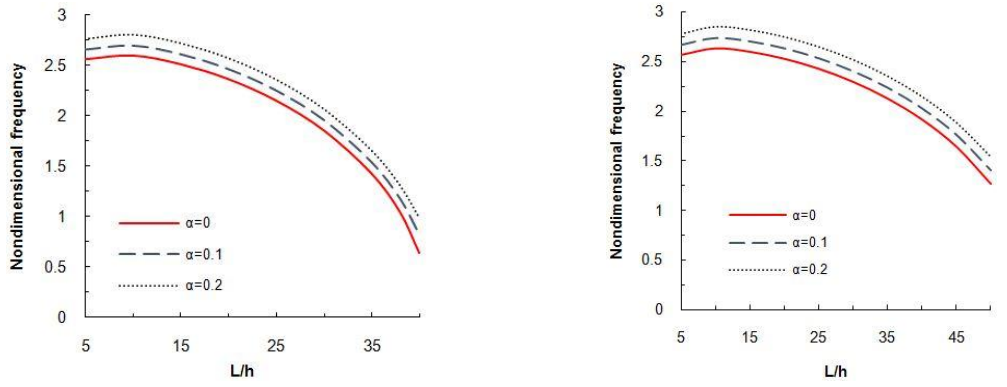

(a) UTR (b) LTR

Fig. 7 The variation of dimensionless frequency of S-S FG porous micro-beam versus slenderness ratiofor various porosity volume fractions (ΔT = 100, $h/l = 2,\ p = 1$).

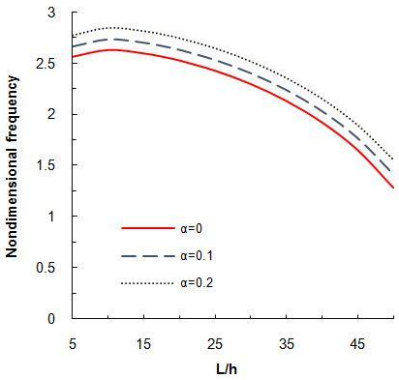

(c) $NLTR$

Fig. 7 Continued

increment of FG microbeams with C-C boundary conditions is more announced than C-S and S-S one. So, effect of porosities on thermal vibration behavior of FG microbeams depends on the type of boundary condition.

In Fig. 7 the variation of the dimensionless frequency of S-S FG porous microbeam with respect to slenderness ratio according to different porosity volume fractions is shown at ΔT = 100, $h/l = 2,\ p = 1$. It can be understand that dimensionless frequency decrease when slenderness ratio increases at a prescribed porosity volume fraction. So, thinner porous FG microbeams have lower frequencies compared to thicker one. Moreover, porosity volume fraction has a same influence on both thick and thin FG microbeams and increases the vibration frequencies.

6. Conclusions

In this paper, thermal vibration of FG microbeams with porosities is examined in framework of a higher order refined beam theory. A modified power-law model is adopted in which the volume fraction of porosities is involved. Hence, the graded material properties of FG microbeam are described according to this model for the first time. Also, different temperature distributions through the thickness direction (*UTR*, *LTR* and *NLTR*) and boundary conditions (S-S, S-C and C-C) are considered in this analysis. An analytical approach is used to solve governing partial differential equations. Numerical results show the following:

- Rising the porosity volume fraction increases the non-dimensional natural frequencies of FG microbeams.
- The non-dimensional frequencies are found to decrease by increasing the power-law index value.
- The natural frequencies are decreased by increasing the thickness-to-length scale parameter. Inclusion of couple stress effect makes the FG beam stiffer, and hence, leads to increment in vibration frequencies regardless of the value of porosity volume fraction that is because of the material properties of the FG microbeams are assumed to vary in the thickness direction.
- For all the boundary conditions, the non-dimensional frequency predicted by NLTR is always greater than those UTR and LTR. So, NLTR and UTR respectively provide the

highest and lowest critical temperatures.

- One significant observation within the range of temperature before the critical temperature is that the FG microbeams with larger values of porosity volume fraction have higher frequency results. But, this trend is opposite in the range of temperature further the critical point. So, larger values of porosity volume fraction provide larger critical temperatures for every type of thermal loading.
- A C-C porous FG microbeam provide larger critical temperatures than S-S one at a constant porosity volume fraction.

References

Aghelinejad, M., Zare, K., Ebrahimi, F. and Rastgoo, A. (2011), "Nonlinear thermomechanical post-buckling analysis of thin functionally graded annular plates based on von-karman's plate theory", *Mech. Adv. Mater. Struct.*, **18**(5), 319-326.

Akgöz, B. and Civalek, Ö. (2013), "Free vibration analysis of axially functionally graded tapered Bernoulli–Euler microbeams based on the modified couple stress theory", *Compos. Struct.*, **98**, 314-322.

Akgöz, B. and Civalek, Ö. (2014), "Thermo-mechanical buckling behavior of functionally graded micro-beams embedded in elastic medium", *Int. J. Eng Sci.*, **85**, 90-104.

Al-Basyouni, K.S., Tounsi, A. and Mahmoud, S.R. (2015), "Size dependent bending and vibration analysis of functionally graded micro beams based on modified couple stress theory and neutral surface position", *Compos. Struct.*, **125**, 621-630.

Ansari, R., Shojaei, M.F. and Gholami, R. (2016), "Size-dependent nonlinear mechanical behavior of third-order shear deformable functionally graded microbeams using the variational differential quadrature method", *Compos. Struct.*, **136**, 669-683.

Asghari, M., Ahmadian, M.T., Kahrobaiyan, M.H. and Rahaeifard, M. (2010), "On the size-dependent behavior of functionally graded micro-beams", *Mater. Des.* (*1980-2015*), **31**(5), 2324-2329.

Asghari, M., Rahaeifard, M., Kahrobaiyan, M.H. and Ahmadian, M.T. (2011), "The modified couple stress functionally graded Timoshenko beam formulation", *Mater. Des.*, **32**(3), 1435-1443.

Barati, M.R., Zenkour, A.M. and Shahverdi, H. (2016), "Thermo-mechanical buckling analysis of embedded nanosize FG plates in thermal environments via an inverse cotangential theory", *Compos. Struct.*, **141**, 203-212.

Dehrouyeh-Semnani, A.M., Mostafaei, H. and Nikkhah-Bahrami, M. (2016), "Free flexural vibration of geometrically imperfect functionally graded microbeams", *Int. J. Eng. Sci.*, **105**, 56-79.

Ebrahimi, F. and Barati, M.R. (2016a), "Temperature distribution effects on buckling behavior of smart heterogeneous nanosize plates based on nonlocal four-variable refined plate theory", *Int. J. Smart Nano Mater.*, **7**(3), 119-143.

Ebrahimi, F. and Barati, M.R. (2016b), "Vibration analysis of smart piezoelectrically actuated nanobeams subjected to magneto-electrical field in thermal environment", *J. Vib. Control*, 1077546316646239.

Ebrahimi, F. and Barati, M.R. (2016c), "Size-dependent thermal stability analysis of graded piezomagnetic nanoplates on elastic medium subjected to various thermal environments", *Appl. Phys. A*, **122**(10), 910.

Ebrahimi, F. and Barati, M.R. (2016d), "Static stability analysis of smart magneto-electro-elastic heterogeneous nanoplates embedded in an elastic medium based on a four-variable refined plate theory", *Smart Mater. Struct.*, **25**(10), 105014.

Ebrahimi, F. and Barati, M.R. (2016e), "Buckling analysis of piezoelectrically actuated smart nanoscale plates subjected to magnetic field", *J. Intel. Mater. Syst. Struct.*, **28**(11), 1472-1490.

Ebrahimi, F. and Barati, M.R. (2016f), "A nonlocal higher-order shear deformation beam theory for vibration analysis of size-dependent functionally graded nanobeams", *Arab. J. Sci. Eng.*, **41**(5), 1679-1690.

Ebrahimi, F. and Barati, M.R. (2016g), "Vibration analysis of smart piezoelectrically actuated nanobeams

subjected to magneto-electrical field in thermal environment", *J. Vib. Control*, 1077546316646239.
Ebrahimi, F. and Barati, M.R. (2017), "Buckling analysis of nonlocal third-order shear deformable functionally graded piezoelectric nanobeams embedded in elastic medium", *J. Brazil. Soc. Mech. Sci. Eng.*, **39**(3), 937-952.
Ebrahimi, F. and Dabbagh, A. (2016), "On flexural wave propagation responses of smart FG magneto-electro-elastic nanoplates via nonlocal strain gradient theory", *Compos. Struct.*, **162**, 281-293.
Ebrahimi, F. and Hosseini, S.H.S. (2016a), "Thermal effects on nonlinear vibration behavior of viscoelastic nanosize plates", *J. Therm. Stresses*, **39**(5), 606-625.
Ebrahimi, F. and Hosseini, S.H.S. (2016b), "Double nanoplate-based NEMS under hydrostatic and electrostatic actuations", *Eur. Phys. J. Plus*, **131**(5), 1-19.
Ebrahimi, F. and Jafari, A. (2016), "A higher-order thermomechanical vibration analysis of temperature-dependent FGM beams with porosities", *J. Eng.*, 2016.
Ebrahimi, F. and Mokhtari, M. (2015), "Transverse vibration analysis of rotating porous beam with functionally graded microstructure using the differential transform method", *J. Brazil. Soc. Mech. Sci. Eng.*, **37**(4), 1435-1444.
Ebrahimi, F. and Rastgo, A. (2008), "An analytical study on the free vibration of smart circular thin FGM plate based on classical plate theory", *Thin-Wall. Struct.*, **46**(12), 1402-1408.
Ebrahimi, F. and Rastgoo, A. (2009), "Nonlinear vibration of smart circular functionally graded plates coupled with piezoelectric layers", *Int. J. Mech. Mater. Des.*, **5**(2), 157-165.
Ebrahimi, F. and Rastgoo, A. (2011), "Nonlinear vibration analysis of piezo-thermo-electrically actuated functionally graded circular plates", *Arch. Appl. Mech.*, **81**(3), 361-383.
Ebrahimi, F. and Zia, M. (2015), "Large amplitude nonlinear vibration analysis of functionally graded Timoshenko beams with porosities", *Acta Astronautica*, **116**, 117-125.
Ebrahimi, F., Naei, M.H. and Rastgoo, A. (2009), "Geometrically nonlinear vibration analysis of piezoelectrically actuated FGM plate with an initial large deformation", *J. Mech. Sci. Technol.*, **23**(8), 2107-2124.
Ebrahimi, F., Barati, M.R. and Dabbagh, A. (2016a), "A nonlocal strain gradient theory for wave propagation analysis in temperature-dependent inhomogeneous nanoplates", *Int. J. Eng. Sci.*, **107**, 169-182.
Ebrahimi, F., Ghasemi, F. and Salari, E. (2016b), "Investigating thermal effects on vibration behavior of temperature-dependent compositionally graded Euler beams with porosities", *Meccanica*, **51**(1), 223-249.
Ghadiri, M. and Shafiei, N. (2016), "Vibration analysis of rotating functionally graded Timoshenko microbeam based on modified couple stress theory under different temperature distributions", *Acta Astronautica*, **121**, 221-240.
Hasanyan, D.J., Batra, R.C. and Harutyunyan, S. (2008), "Pull-in instabilities in functionally graded micro-thermoelectromechanical systems", *J. Therm. Stresses*, **31**(10), 1006-1021.
Ke, L.L., Wang, Y.S., Yang, J. and Kitipornchai, S. (2012), "Nonlinear free vibration of size-dependent functionally graded microbeams", *Int. J. Eng. Sci.*, **50**(1), 256-267.
Kiani, Y. and Eslami, M.R. (2013), "An exact solution for thermal buckling of annular FGM plates on an elastic medium", *Compos. Part B: Eng.*, **45**(1), 101-110.
Lee, C.Y. and Kim, J.H. (2013), "Hygrothermal postbuckling behavior of functionally graded plates", *Compos. Struct.*, **95**, 278-282.
Lü, C.F., Lim, C.W. and Chen, W.Q. (2009), "Size-dependent elastic behavior of FGM ultra-thin films based on generalized refined theory", *Int. J. Solids Struct.*, **46**(5), 1176-1185.
Şimşek, M. and Kocatürk, T. (2009), "Free and forced vibration of a functionally graded beam subjected to a concentrated moving harmonic load", *Compos. Struct.*, **90**(4), 465-473.
Şimşek, M. and Reddy, J.N. (2013), "Bending and vibration of functionally graded microbeams using a new higher order beam theory and the modified couple stress theory", *Int. J. Eng. Sci.*, **64**, 37-53.
Şimşek, M., Kocatürk, T. and Akbaş, Ş.D. (2013), "Static bending of a functionally graded microscale Timoshenko beam based on the modified couple stress theory", *Compos. Struct.*, **95**, 740-747.
Thai, H.T. and Vo, T.P. (2012), "Bending and free vibration of functionally graded beams using various higher-order shear deformation beam theories", *Int. J. Mech. Sci.*, **62**(1), 57-66.

Wattanasakulpong, N. and Ungbhakorn, V. (2014), "Linear and nonlinear vibration analysis of elastically restrained ends FGM beams with porosities", *Aerosp. Sci. Technol.*, **32**(1), 111-120.
Wattanasakulpong, N., Prusty, B.G., Kelly, D.W. and Hoffman, M. (2012), "Free vibration analysis of layered functionally graded beams with experimental validation", *Mater. Des.* (*1980-2015*), **36**, 182-190.
Yang, F.A.C.M., Chong, A.C.M., Lam, D.C.C. and Tong, P. (2002), "Couple stress based strain gradient theory for elasticity", *Int. J. Solids Struct.*, **39**(10), 2731-2743.

CC